23rd International Conference on Modelling and Applied Simulation, 020
21st International Multidisciplinary Modeling & Simulation Multiconference

2724-0037 © 2024 The Authors.
doi: 10.46354/i3m.2024.mas.020

Stress-Driven Simulation model in Polar Coordinates: The Analytical case for Circular Plates

Roberto Cianci[1], Agostino G. Bruzzone[1,*], Roberta Sburlati[1] and Mohamadreza Jafarinezhad[1]

[1] University of Genoa, Italy

[*] Corresponding author. Email address: agostino@itim.unige.it

Abstract

This study aims to analyze a circular plate with specific characteristics. The plate has an outer radius and thickness (h). An approach is introduced to simulate the stress-driven theory based on Kirchhoff plate assumptions. The differential equations for the circular plate are obtained in Cartesian coordinates and then moved to polar coordinates. When R is going to infinity, the equation is solved analytically. We found that the displacement on the lateral surface is depending by the nonlocal parameter, while resultant moments are unaffected. A finite element solution is presented by using the Galerkin technique, for the case of a solid circular plate with clamped boundary conditions in the outer radius R. We present a comparison between the newly stress-driven theory and a previous formulation. So doing we get that both formulations predict a reduction in transversal displacement with an increase in the nonlocal parameter. The reduction is more pronounced in the former theory compared to the refined theory.

Keywords: Nonlocal elasticity, Analytical solution, Simulation, Strategos techniques, Functionally graded materials (FGMs)

1. Introduction

The application of nanostructures and nano-systems has been emerging rapidly in recent years in various disciplines, such as mechanical, civil, electrical, and medical engineering. In conjunction with the increased applications of functionally graded materials (FGMs) in engineering fields, the analysis of nano FGM plates as a component of the structures has great significance (Witvrouw and Mehta, 2005).

In the framework of analytical solution for static analysis, Duan and Wang (2007) present an exact solution for the axisymmetric bending of circular plates based on the Eringen nonlocal theory. They found that the small-scale effect enables larger deflections, bending moments, shear force, and lower bending stiffness compared to the local plate. Using Eringen's nonlocal theory, Yükseler (2020) found the exact solution for the bending problem of circular plates subjected to uniformly distributed loads with a concentrated nonlocal force. Concerning strain gradient theory, from the analytical solution provided by (Gousias and Lazopoulos, 2015), Barretta et al. (2019) conclude that for simply-supported circular plates subjected to uniformly distributed bending couples along the boundary, the transverse deflection of the nanoplate is independent of the scale parameter. Utilizing the stress-driven theory, the exact solutions for a Timoshenko nano-beam with cantilevered, clamped, and simply supported boundary conditions are given in (Barretta et al., 2018). Considering the afore-cited contributions, in some specific loading and boundary conditions, neither Eringen nor strain gradient theory are able to interpret the influence of size-dependent effects. Thus, this paper considers the

stress-driven theory to formulate the static and free vibration analysis of functionally graded annular plates.

2. Theoretical formulations

An annular FGM plate with an inner radius a, outer radius b, and thickness h, as shown in Fig. 1 is considered in this study.

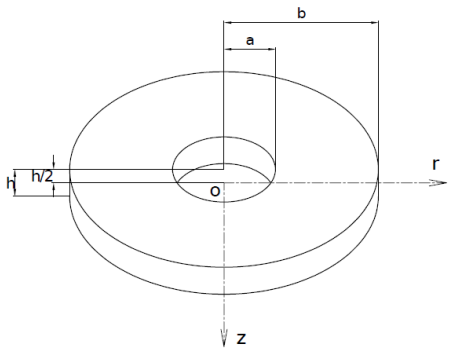

Figure 1: The annular plate

An annular FGM plate with an inner radius a, outer radius b, and thickness h, as shown in Fig. 1 is considered in this study.

2.1. Material properties of FGM plate

The material properties change gradually in the thickness direction as a function of location. According to a power-law distribution function, the volume fraction of two different materials, for example, ceramic (c) and metal (m), is:

$$V(z) = \left(\frac{2z+h}{2h}\right)^{\xi} \tag{1}$$

and the effective material property P(z) is expressed as:

$$P(z) = P_m + (P_c - P_m)\,V(z) \tag{2}$$

where P could be any of the FGM properties and ξ is the power-law index. Here, P_c and P_m are the related properties of the two different constituent materials, respectively. Fig. 2 shows changes in the volume fraction across the plate thickness for different heterogeneity parameter values ξ.

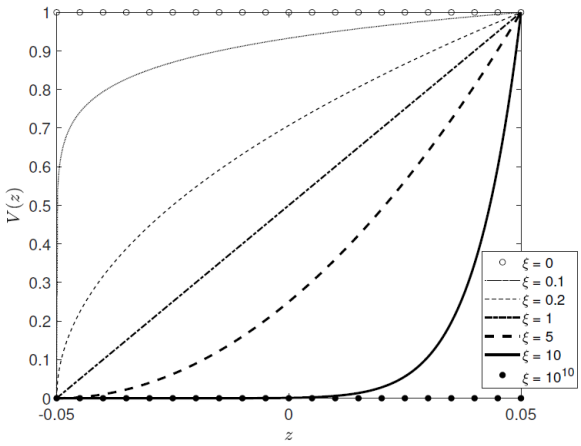

Figure 2: Changes in the volume fraction for different values of ξ across the thickness

2.2. Mathematical model for FGM plate

Based on the classical bending Kirchhoff's plate theory in the axisymmetric case, the displacement fields are:

$$u_r(r,z,t) = -z\frac{\partial}{\partial r}w(r,t)\,, \quad u_\theta(r,z,t) = 0, \quad u_z(r,z,t) = w(r,t) \tag{3}$$

where w(r, t) is the transversal deflection. The strain-displacement relationships in the elasticity theory are given as

$$\epsilon_{rr}(r,z,t) = \frac{\partial}{\partial r}u_r(r,z,t)\,, \quad \epsilon_{\theta\theta}(r,z,t) = \frac{1}{r}u_r(r,z,t) \tag{4}$$

Substituting Eq. 3 in Eq. 4, the strains may be written as

$$\epsilon_{rr}(r,z,t) = -z\frac{\partial^2}{\partial r^2}w(r,t)\,, \quad \epsilon_{\theta\theta}(r,z,t) = -\frac{z}{r}\frac{\partial}{\partial r}w(r,t) \tag{5}$$

According to Hooke's law, concerning plane stress assumption, stress-strain relations for a locally isotropic graded material variable in the thickness of the plate, the linear elastic FGM equations are

$$\begin{Bmatrix} \sigma_{rr} \\ \sigma_{\theta\theta} \end{Bmatrix} = \frac{E(z)}{1-\nu^2}\begin{bmatrix} 1 & \nu \\ \nu & 1 \end{bmatrix}\begin{Bmatrix} \epsilon_{rr} \\ \epsilon_{\theta\theta} \end{Bmatrix} \tag{6}$$

where only Young's modulus is variable, and Poisson's ratio is assumed to be constant. This hypothesis is assumed since, on the one hand, there are results in the literature that numerically show the limitate influence of Poisson's ratio in the elastic response (see, e.g., (Sburlati et al., 2014)). On the other hand, considering variation in Poisson's ratio leads to more complexity in the governing equation and in the search of its analytical solution.

For the plate, the moment and resultant shear forces are defined as:

$$M_{rr}(r,t) = \int_{-\frac{h}{2}}^{+\frac{h}{2}} \sigma_{rr}(r,z,t)\,z dz, \quad M_{\theta\theta}(r,t) = \int_{-\frac{h}{2}}^{+\frac{h}{2}} \sigma_{\theta\theta}(r,z,t)\,z dz \tag{7}$$

$$Q_r(r,t) = \frac{\partial}{\partial r} M_{rr}(r,t) + \frac{1}{r}\left(M_{rr}(r,t) - M_{\theta\theta}(r,t)\right) \tag{8}$$

By defining curvature in the plate at a given point on the middle plane as

$$k_{rr} = -\frac{\partial^2}{\partial r^2} w(r,t)\,, \quad k_{\theta\theta} = -\frac{1}{r}\frac{\partial}{\partial r} w(r,t) \tag{9}$$

and using Eqs. 6, 5 we obtain:

$$M_{rr}(r,t) = D^\star\left(k_{\theta\theta}(r,t)\,\nu + k_{rr}(r,t)\right), \quad M_{\theta\theta}(r,t) = D^\star\left(k_{rr}(r,t)\,\nu + k_{\theta\theta}(r,t)\right) \tag{10}$$

where the flexural rigidity of the plate D⋆ is:

$$D^\star = \frac{1}{1-\nu^2}\int_{-\frac{h}{2}}^{+\frac{h}{2}} E(z) z^2 dz \tag{11}$$

We remark that the FGM behavior of the material is relevant to the calculation of this term.

In deriving the governing differential equation of motion, we consider the expression of plate theory expressed in the form: (Reddy, 2006)

$$\begin{aligned}&\frac{1}{r}\left(\frac{\partial^2}{\partial r^2}\left(r M_{rr}(r,t)\right) - \frac{\partial}{\partial r} M_{\theta\theta}(r,t)\right)\\ &= -p(r,t) + I_0\frac{\partial^2}{\partial t^2} w(r,t) - I_2\frac{\partial^2}{\partial t^2}\left(\frac{\partial^2}{\partial r^2} w(r,t) + \frac{1}{r}\frac{\partial}{\partial r} w(r,t)\right)\end{aligned} \tag{12}$$

we have denoted the mass moments of inertia are:

$$I_0 = \int_{-\frac{h}{2}}^{+\frac{h}{2}} \rho(z) dz, \quad I_2 = \int_{-\frac{h}{2}}^{+\frac{h}{2}} \rho(z) z^2 dz \tag{13}$$

where ρ(z) is the mass density of the FG material and p(r, t) is a transversal axisymmetric load.

2.3. Nonlocal governing equations

Inspired by (Romano and Barretta, 2017), we use the stress-driven nonlocal theory (SDT) to capture the size effects in the axisymmetric functionally graded annular plate.

To this end, the local curvatures in a functionally graded annular plate are calculated. Applying the stress-driven integral constitutive law, the nonlocal elastic curvature is obtained as a convolution between the local elastic curvature and the bi-exponential kernel.

According to stress-driven nonlocal theory, the elastic strain ϵ at a point r of Γ is a convolution of the local stress σ with an averaging kernel ϕ_λ

$$\epsilon(r) = \int_\Gamma \phi_\lambda(r-\rho)\, C\sigma(\rho)\, d\rho \tag{14}$$

where C is the local elastic compliance.

We write Eq. 10 in terms of the local bending curvatures as:

$$k_{rr}(r,t) = \frac{M_{rr}(r,t) - \nu M_{\theta\theta}(r,t)}{D^\star(1-\nu^2)}, \quad k_{\theta\theta}(r,t) = \frac{M_{\theta\theta}(r,t) - \nu M_{rr}(r,t)}{D^\star(1-\nu^2)} \tag{15}$$

with reference to Eqs. 5, 9, 14, and 15, we impose that the nonlocal elastic curvature χel is

an integral convolution of the local radial curvature and a smoothing kernel function ϕ_λ to formulate the SDT nonlocal integral model in axisymmetric cylindrical coordinates (Barretta et al., 2019).

$$\chi_{el}(r,t) = \int_a^b \phi_\lambda(r-\rho)\frac{M_{rr}(\rho,t) - \nu M_{\theta\theta}(\rho,t)}{D^\star(1-\nu^2)} d\rho \tag{16}$$

where ϕ_λ is:

$$\phi_\lambda(r) = \frac{1}{2L_c} e^{-\frac{|r|}{L_c}} \tag{17}$$

$$\lambda = \frac{L_c}{b-a} \tag{18}$$

Here λ is a positive parameter depending on the characteristic length Lc, which reflects the size effect. In view of Eq. 17, equation 16 is a particular case of the general integral form:

$$\int_a^b e^{\zeta|\rho - r|} y(\rho,t)\, d\rho = f(r,t)\,. \tag{19}$$

According to (Polyanin and Manzhirov, 2008) (see section 3.2), the integral formulation of Eq. 19 is reformed to a differential equation with constitutive boundary conditions in the following form

$$\chi_{el}(r,t) - L_c^2\frac{\partial^2}{\partial r^2}\chi_{el}(r,t) = \frac{M_{rr}(r,t) - \nu M_{\theta\theta}(r,t)}{D^\star(1-\nu^2)} \tag{20}$$

$$\frac{\partial}{\partial r}\chi_{el}(a,t) - \frac{1}{L_c}\chi_{el}(a,t) = 0, \quad \frac{\partial}{\partial r}\chi_{el}(b,t) + \frac{1}{L_c}\chi_{el}(b,t) = 0 \tag{21}$$

Now the moment M_{rr} and $M_{\theta\theta}$ is obtained by solving Eqs. 20 and 152 in terms of nonlocal bending curvatures; then recalling the kinematic compatibility (i.e., $\chi_{tot} = -\partial^2 w/\partial r^2$), the results in terms of displacement are computed:

$$\begin{aligned}M_{rr}(r,t) &= D^\star\left(L_c^2\frac{\partial^4}{\partial r^4} w(r,t) - \frac{\nu}{r}\frac{\partial}{\partial r} w(r,t) - \frac{\partial^2}{\partial r^2} w(r,t)\right)\\ M_{\theta\theta}(r,t) &= D^\star\left(\nu L_c^2\frac{\partial^4}{\partial r^4} w(r,t) - \nu\frac{\partial^2}{\partial r^2} w(r,t) - \frac{1}{r}\frac{\partial}{\partial r} w(r,t)\right)\end{aligned} \tag{22}$$

Finally, by combining Eq. 12 and Eq. 22, the nonlocal stress-driven formulation of Kirchhof's plate model is obtained:

$$D^\star\left(\left(\frac{\partial^6}{\partial r^6} w(r,t) - \frac{(\nu-2)}{r}\frac{\partial^5}{\partial r^5} w(r,t)\right) L_c^2 - \Delta^2 w(r,t)\right) = \left(I_0 - I_2\Delta\right)\frac{\partial^2}{\partial t^2} w(r,t) - p(r,t) \tag{23}$$

where Δ is the Laplace operator in axisymmetric polar coordinates.

For the static analysis Eq. 23 is reduced to the equation:

$$D^\star\left(L_c^2\left(\frac{d^6}{dr^6} - \frac{(\nu-2)}{r}\frac{d^5}{dr^5}\right) - \frac{d^4}{dr^4} - \frac{2}{r}\frac{d^3}{dr^3} + \frac{1}{r^2}\frac{d^2}{dr^2} - \frac{1}{r^3}\frac{d}{dr}\right) w(r) = -p(r) \tag{24}$$

For the axisymmetric free vibration analysis, by introducing the pulses ω_n, we write:

$$w(r,t) = e^{i\omega_n t}\widetilde{w}(r) \tag{25}$$

so Eq. 23 becomes:

$$- D^{\star}\left(\frac{d^4}{dr^4}+\frac{2}{r}\frac{d^3}{dr^3}-\frac{1}{r^2}\frac{d^2}{dr^2}+\frac{1}{r^3}\frac{d}{dr}-L_c^2\left(\frac{d^6}{dr^6}-\frac{(\nu-2)}{r}\frac{d^5}{dr^5}\right)\right)\widetilde{w}(r) + \omega_n^2\left(I_0-I_2\left(\frac{d^2}{dr^2}-\frac{1}{r}\frac{d}{dr}\right)\right)\widetilde{w}(r)=0. \quad (26)$$

3. Analytical solution for the static analysis

In this section, we study the six-order equation 24 from an analytical point of view to obtain a closed-form solution. Since equation 24 is non-homogeneous, in order to determine its general integral, we first consider the associate homogeneous equation:

$$L_c^2\frac{d^6}{dr^6}w(r)-\frac{(\nu-2)L_c^2}{r}\frac{d^5}{dr^5}w(r)-\frac{d^4}{dr^4}w(r)-\frac{2}{r}\frac{d^3}{dr^3}w(r)+\frac{1}{r^2}\frac{d^2}{dr^2}w(r)-\frac{1}{r^3}\frac{d}{dr}w(r)=0 \quad (27)$$

To solve this equation, we firstly remark that, by defining the term

$$H(r)=2r^2L_c^2\frac{d^4}{dr^4}w(r)-2rL_c^2(\nu+1)\frac{d^3}{dr^3}w(r)+\left(2(\nu+1)L_c^2-2r^2\right)\frac{d^2}{dr^2}w(r)+2r\frac{d}{dr}w(r) \quad (28)$$

one gets that Eq. 27 gives:

$$\frac{d^2}{dr^2}H(r)-\frac{1}{r}\frac{d}{dr}H(r)=0. \quad (29)$$

This equation is easily integrated, and so one gets the following equation:

$$2r^2L_c^2\frac{d^4}{dr^4}w(r)-2rL_c^2(\nu+1)\frac{d^3}{dr^3}w(r)+2\left((\nu+1)L_c^2-2r^2\right)\frac{d^2}{dr^2}w(r)+2r\frac{d}{dr}w(r)=k_1+k_2r^2 \quad (30)$$

This non-homogeneous fourth-order equation is solved in terms of special functions (Abramowitz and Stegun, 1964). By renaming the integration constants, we write the expression of the general integral of Eq. 27 in the form:

$$\begin{aligned} w(r) &= C_1r^2+C_2+C_3r^3{}_2F_3\left(\frac{1}{2},\frac{3}{2};2,\frac{5}{2},1-\frac{\nu}{2};\frac{r^2}{4L_c^2}\right) \\ &+C_4r^{3+\nu}{}_2F_3\left(\frac{1}{2}+\frac{\nu}{2},\frac{3}{2}+\frac{\nu}{2};1+\frac{\nu}{2},2+\frac{\nu}{2},\frac{5}{2}+\frac{\nu}{2};\frac{r^2}{4L_c^2}\right) \\ &+C_5r^4{}_3F_4\left(1,1,2;\frac{3}{2},\frac{5}{2},3,\frac{3}{2}-\frac{\nu}{2};\frac{r^2}{4L_c^2}\right)+C_6r^3G^{2,2}_{2,4}\left(\frac{r^2}{4L_c^2}\middle|_{0,-1,-\frac{3}{2},\frac{\nu}{2}}^{-\frac{1}{2},\frac{1}{2}}\right) \end{aligned} \quad (31)$$

where ${}_2F_3(a1, a2; b1, b2, b3; z)$ and ${}_3F_4(a1, a2, a3; b1, b2, b3, b4; z)$ denote hypergeometric functions and

$$G^{2,2}_{2,4}\left(\frac{r^2}{4L_c^2}\middle|_{b_1,b_2,b_3,b_4}^{a_1,a_2}\right)$$

a Meijer G-function.

For the convenience of the reader wishing to check this result, we recall that the differential equation verified by the Meijer G-function term:

$$s(r)=r^3G^{2,2}_{2,4}\left(\frac{r^2}{4L_c^2}\middle|_{0,-1,-\frac{3}{2},\frac{\nu}{2}}^{-\frac{1}{2},\frac{1}{2}}\right)$$

is:

$$r\frac{d}{dr}s(r)+\left(L_c^2\nu+L_c^2-r^2\right)\frac{d^2}{dr^2}s(r)-rL_c^2(\nu+1)\frac{d^3}{dr^3}s(r)+r^2L_c^2\frac{d^4}{dr^4}s(r)=0. \quad (32)$$

By using this result and the generalized hypergeometric differential equation (Abramowitz and Stegun, 1964), one is able to verify that the general integral of Eq. 27 is Eq. 31. Now, if we consider the constant loading term $p(r) = p$, in Eq. 24 we have to add the term:

$$w(r)=\frac{p\,r^4}{64D^{\star}} \quad (33)$$

So, the general integral of Eq. 24 is obtained.

To uniquely get the explicit solutions, we must determine the six integration constants *C1, . . . ,C6* from the specific boundary conditions. This is possible since, further to the standard Cauchy theory requirements, we have to take into account also the two conditions furnished by Eqs. 21.

In such a way, we shall get, for each case, a unique solution by solving a not homogeneous system of six linear equations in six conditions.

4. Results and Discussion

Homogeneous materials and functionally graded materials in the thickness of the plate are considered. For FGM nanoplate, we consider constant Poisson's ratio and the following power law for the Young modulus and density.

$$\begin{aligned} E(z) &= E_m+(E_c-E_m)\left(\frac{2z+h}{2h}\right)^{\xi} \\ \rho(z) &= \rho_m+(\rho_c-\rho_m)\left(\frac{2z+h}{2h}\right)^{\xi} \end{aligned} \quad (34)$$

where subscripts *m* and *c* refer to metal and ceramic constituents, respectively. To compare our findings with those of the reference, we adopted the material properties from Shishesaz et al. (2022). The material properties are given in the table 1.

E_c (Gpa)	E_m (Gpa)	$\rho_c(\mathrm{kg}/m^3)$	ρ_m (kg/m^3)
380	211	3600	7860

Table 1: Material properties (Shishesaz et al., 2022)

For homogeneous and FGM plates, in the next subsections, we consider static and dynamic analyses for the annular nanoplate with two different boundary conditions (BCs) equal in inner and outer radii: simply supported (S-S) edges and clamped (C-C) edges.

For the S-S nanoplate we assume:

$$\begin{aligned} w(a,t)=0, \quad M_{rr}(a,t)=0 \\ w(b,t)=0, \quad M_{rr}(b,t)=0 \end{aligned} \quad (35)$$

and for C-C nanoplate we assume:

$$\begin{aligned} w(a,t)=0, \quad \frac{dw(a,t)}{dr}=0 \\ w(b,t)=0, \quad \frac{dw(b,t)}{dr}=0 \end{aligned} \quad (36)$$

Further, we also have to consider the constitutive boundary conditions Eq. 21:

$$\frac{d^3w(a,t)}{dr^3}+\frac{1}{L_c}\frac{d^2w(a,t)}{dr^2}=0$$
$$\frac{d^3w(b,t)}{dr^3}-\frac{1}{L_c}\frac{d^2w(b,t)}{dr^2}=0 \quad (37)$$

in terms of transversal displacement.

The different characteristic parameter values (λ) allow us to evaluate the nano-scale effects given by the NLT.

The numerical results are also compared with results obtained in the literature.

4.1. Analytical results

To assess the impact of characteristic parameter λ on the results, we set ξ = 0 - the homogeneous 'ceramic' case - and change the value of λ. By assuming *b = 1*, *a = b/3*, *h = b/10*, and *ν = 1/4*, results are obtained in the following normalized form; the maximum transversal displacement

$$\bar{w}^{max} = w_{NLT}^{max}/w_{LT}^{max},$$

the transversal displacement

$$\bar{w}(r) = w(r)/w_{LT}^{max},$$

the resultant radial moment

$$\bar{M}_{rr}(r) = M_{rr}(r)/M_{rr}{}_{LT}^{max},$$

and the hoop moment

$$\bar{M}_{\theta\theta}(r) = M_{\theta\theta}(r)/M_{\theta\theta}{}_{LT}^{max}.$$

The notation $(\dots)_{LT}^{max}$ denotes the maxim value of the previous quantities when LT is taken into account.

4.1.1. Effects of the nonlocal parameter in different boundary conditions

The following figures, the size effect is studied in a plate with clamped and simply supported boundary conditions. Figure 3 compares the normalized transversal displacement of the annular plate for ranges of λ. The pattern for clamped BC is the same as simply supported BC: a reduction in plate displacement is seen with the increase of λ, which means that the nonlocal model predicts stiffening behavior. The lowest deflection value is for λ = 1, which is quite a lot smaller than the value for λ = 0, specifically for clamped BC.

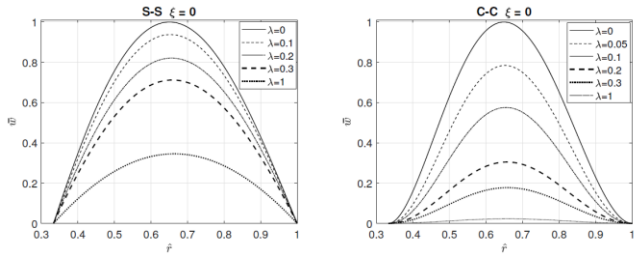

Figure 3: The effect of characteristic parameter λ on the deflection of the clamped and simply supported annular plate by considering ξ = 0

Figure 4 illustrates the variation of radial moments according to changes in the variable λ. The main facts that stand out are that for a simply supported plate, the radial moment is always positive, and the values increase with the increase of λ. In clamped BC, the radial moment is negative at the boundaries and becomes positive as we distance from the edges. As λ increases, the maximum positive value of radial moment $(\bar{M}_{rr}{}^{max})$ initially decreases but later roses. Also, curves associated with different values of λ intersect.

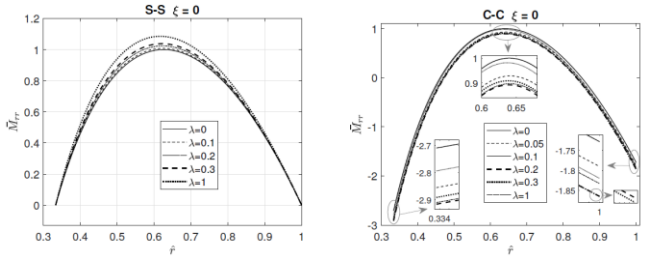

Figure 4: The effect of characteristic parameter λ on the radial moment of the simply supported and clamped annular plate by considering ξ = 0

Figure 5 indicates the effects of λ on the hoop moment values. Increasing the magnitude of λ in a simply supported plate reduces the hoop moment. The hoop moment for λ = 0 is outstripped by a narrow margin in comparison with the small values of λ (e.g., λ = 0.1).

However, the distinctions become more pronounced regarding greater λ. In clamped BC, as λ increased, $\bar{M}_{\theta\theta}{}^{max}$ max dropped, then rose. It is also obvious that in both simply supported and clamped BCs, by increasing λ, the radial point, in which the hoop moment becomes zero, approaches the inner radius.

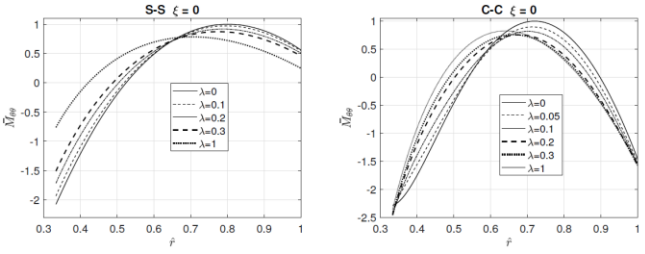

Figure 5: The effect of characteristic parameter λ on the

hoop moment of the simply supported and clamped annular plate by considering ξ = 0

5. Conclusions

The present study investigates the static and free vibration analysis of an FGM annular plate. The governing equations are derived based on the stress-driven nonlocal theory. The analytical solution for the static case is obtained in the section 3.

Regarding simply supported annular plate, increasing λ results in an increase of the radial moment but a decrease in the hoop moment.

Considering clamped BC, both $\bar{M}_{\theta\theta}{}^{max}$ and $\bar{M}_{rr}{}^{max}$ decline then soar as λ increased. In contrary, the variation of $\bar{M}_{rr}{}^{max}$ and $\bar{M}_{\theta\theta}{}^{max}$ is vise versa.

References

Abramowitz, M. and Stegun, I. A. (1964). Handbook of mathematical functions with formulas, graphs, and mathematical tables, volume 55. US Government printing office.

Barretta, R., Faghidian, S. A., and De Sciarra, F. M. (2019). Stress-driven nonlocal integral elasticity for axisymmetric nano-plates. International Journal of Engineering Science, 136:38-52.

Barretta, R., Luciano, R., de Sciarra, F. M., and Ruta, G. (2018). Stress-driven nonlocal integral model for timoshenko elastic nano-beams. European Journal of Mechanics-A/Solids, 72:275-286.

Duan, W. andWang, C. M. (2007). Exact solutions for axisymmetric bending of micro/nanoscale circular plates based on nonlocal plate theory. Nanotechnology, 18(38):385704.

Gousias, N. and Lazopoulos, A. (2015). Axisymmetric bending of strain gradient elastic circular thin plates. Archive of Applied Mechanics, 85(11):1719-1731.

Polyanin, A. D. and Manzhirov, A. V. (2008). Handbook of integral equations. Chapman and Hall/CRC.

Reddy, J. N. (2006). Theory and analysis of elastic plates and shells. CRC press.

Romano, G. and Barretta, R. (2017). Nonlocal elasticity in nanobeams: the stress-driven integral model. International Journal of Engineering Science, 115:14-27.

Sburlati, R., Atashipour, S. R., and Atashipour, S. A. (2014). Reduction of the stress concentration factor in a homogeneous panel with hole by using a functionally graded layer. Composites Part B: Engineering, 61:99-109.

Shishesaz, M., Shariati, M., and Hosseini, M. (2022). Size-effect analysis on vibrational response of functionally graded annular nano-plate based on nonlocal stress-driven method. International Journal of Structural Stability and Dynamics, page 2250098.

Witvrouw, A. and Mehta, A. (2005). The use of functionally graded poly-sige layers for mems applications. In Materials science forum, volume 492, pages 255-260. Trans Tech Publ.

Yükseler, R. F. (2020). Exact nonlocal solutions of circular nanoplates subjected to uniformly distributed loads and nonlocal concentrated forces. Journal of the Brazilian Society of Mechanical Sciences and Engineering, 42(1):1-10.